

AD-A159 382

DYNAMIC FRACTURE TOUGHNESS(U) WASHINGTON UNIV SEATTLE  
DEPT OF MECHANICAL ENGINEERING A S KOBAYASHI ET AL.  
AUG 85 UWA/DME/TR-85/53 N00014-85-K-0187

1/1

UNCLASSIFIED

F/G 11/6

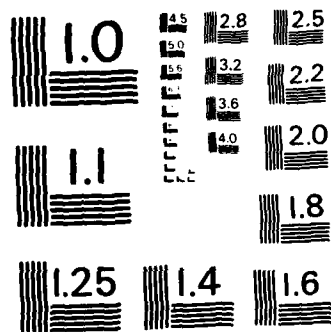
NL



END

FORM 10

010



MICROCOPY RESOLUTION TEST CHART  
NATIONAL BUREAU OF STANDARDS-1963-A

(2)

Office of Naval Research

Contract N00014-85-K-0187 *OK*

Technical Report No. UWA/DME/TR-85/53

DYNAMIC FRACTURE TOUGHNESS

by

A. S. Kobayashi, M. Ramulu, M. S. Dadkhah, K.-H. Yang and B. S.-J. Kang

August 1985

The research reported in this technical report was made possible through support extended to the Department of Mechanical Engineering, University of Washington, by the Office of Naval Research under Contract N00014-85-K-0187. Reproduction in whole or in part is permitted for any purpose of the United States Government.

**DISTRIBUTION STATEMENT A**

Approved for public release;  
Distribution Unlimited

*W*  
**DTIC  
ELECTE**

**S** SEP 25 1985 **D**

**B**

Department of Mechanical Engineering

College of Engineering

University of Washington

AD-A159 382

DTIC FILE COPY

## Dynamic Fracture Toughness

A. S. Kobayashi, M. Ramulu, M. S. Dadkhah, K.-H. Yang and B. S.-J. Kang  
University of Washington  
Department of Mechanical Engineering  
Seattle, Washington 98195

### ABSTRACT

Dynamic fracture toughness versus crack velocity relations of Homalite-100, polycarbonate, hardened 4340 steel and reaction bonded silicon nitride are reviewed and discrepancies with published data and their probable causes are discussed. Data scatter in published data are attributed in part to the observed fluctuations in crack velocities. The results reaffirmed our previous conclusion that the dynamic fracture toughness versus crack velocity relation is specimen dependent and that the dynamic crack arrest stress intensity factor is not a unique material property.

### INTRODUCTION

Since Wells and Post [1], with the help of Irwin [2], determined the crack driving force, i.e. the dynamic stress intensity factor, and the crack velocity in fracturing photoelastic plates, numerous attempts have been made to relate these two quantities. The dynamic fracture community's interest in this relation is demonstrated by the fact that six out of the seven review papers dealing with the experimental aspects of dynamic fracture mechanics in the recent issue of the International Journal of Fracture [3] refer to the uniqueness or lack thereof in the dynamic stress intensity factor versus crack velocity relation and/or in the dynamic crack arrest stress intensity factor. The survey paper by Dally et al [4] describes the major findings to date and

indicates possible sources of experimental errors which may have lead to the current controversies on this subject.

The purpose of this paper is to present additional experimental results, some of which were obtained by the authors and their colleagues over the past decade, on dynamic stress intensity factor versus crack velocity relations in the context of the current controversy. Throughout this paper, the measured/computed dynamic stress intensity factors are referred to as the dynamic fracture toughness. Thus the driving force, i.e. the dynamic stress intensity factor, is tacitly equated to the material resistance to dynamic crack growth, i.e. dynamic fracture toughness.

#### DYNAMIC PHOTOELASTIC RESULTS

Although photoelastic polymers, such as Homalite-100 and epoxy, are not primary structural material, dynamic photoelasticity and caustics have been used in the past decade and half to uncover the basic principles which govern dynamic fracture mechanics. The dynamic fracture toughness,  $K_{ID}$ , versus crack velocity,  $\dot{a}$ , relations, which have been obtained through extensive fracture testing of polymers, showed that the the terminal crack velocity is test specimen dependent while the "near vertical stem" of these relations is either a unique [5] or a nonunique [6,7] material property. The latter is in agreement with the conclusion derived by one of the authors several years ago [8,9]. The dynamic photoelastic data used to support this conclusion has been reevaluated in this paper by an updated data processing procedure which incorporates higher order terms of the dynamic crack tip stress field.

Figures 1 and 2 show the  $K_{ID}$  versus  $\dot{a}$  relations for Homalite-100 and polycarbonate fracture specimens. No attempt was made to fit an average  $K_{ID}$  versus  $\dot{a}$  curve through the wide scatter of data generated from various batches of Homalite-100 and polycarbonate sheets tested over a period of ten years.

Figure 1 shows that the scatter bands about the imagined vertical stems of the dynamic tear test (DTT), single edge notched (SEN), modified compact (M-CT) and wedge-loaded rectangular double cantilever beam (WL-RDCB) Homalite-100 specimens are similar to those shown in [7]. However, differences in the minimum dynamic fracture toughness,  $K_{Im}$ , of the vertical stems of the DTT and SEN specimens are larger than that reported in [6]. The difference in  $K_{Im}$  for the more ductile WL-RDCB and DTT polycarbonate specimens is about 10 percent and is in agreement with the general observation by Rosakis et al [10].

Figure 3 shows the  $K_{ID}$  versus crack extension relations of four SEN specimens subjected to different fixed grip loading condition [9]. Also shown are the corresponding static stress intensity factor. This figure, which is similar to the well-publicized results of Kalthoff et al [11], demonstrates that the dynamic crack arrest stress intensity factor,  $K_{Ia}^{dym}$ , is a constant for the same specimen while the static crack arrest intensity factor,  $K_{Ia}^{stat}$ , varies with the crack initiation condition.

#### SCATTER IN $K_{ID}$ VERSUS $\dot{a}$ RELATION

Since the above photoelastic results are in general agreement with the caustic results, the published discrepancies in the  $K_{ID}$  versus  $\dot{a}$  results cannot be attributed to the differences in the experimental procedures alone. However, the discrepancies could be attributed in part to the size of the crack tip region used for data reduction in the presence of stress wave effects [12]. The caustic method by definition and the authors' photoelastic method by choice had restricted the crack tip region to within 5 mm of the crack tip but outside of the nonlinear region of about 1 mm [13] surrounding the crack tip. The dynamic photoelastic results in [4] are derived from larger crack tip regions with the use of larger number of higher order terms in the crack tip stress



A-1

field. Such data reduction procedure will yield accurate stress intensity factors under static loading. On the otherhand, the dynamic isochromatics in a larger crack tip region would be less sensitive to small perturbations in the dynamic stress intensity factor as shown in a previous numerical experiment [8]. The combined effect of the large crack tip region, in which measurements were made, and the large fracture specimens [4], which are shown in the right half of Figure 4, would minimize any oscillations in the  $K_{ID}$ . In contrast, the stress wave effect is more severe in the smaller fracture specimens, which is shown in the left half of Figure 4, and the resultant oscillations in  $K_{ID}$  is more readily detected when a smaller crack tip region is used in data reduction.

The experimental errors involved in crack velocity measurements have been discussed in [4,12,15] with [4] suggesting the use of ultrasonic fractography [16] for increased accuracy. Such crack velocity measurements [17] were made on CT, SEN, 3-point bend and Charpy polymethyl methacrylate (PMMA) specimens approximately one half the size of the smallest WL-RDCB specimen in Figure 4. The qualitative changes in the crack velocities with crack extension in the SEN, CT and 3-point bend specimens are similar to those reported in [18,19,20], respectively. Moreover, the crack velocities, which were determined from the discrete Cranz-Schardin photographs, ultrasonic fractography and streaking photography did not exhibit any unusual perturbation in the otherwise gradually varying crack velocities in these polymeric materials. Figure 5 shows the experimental setup and a typical streaking photograph [19] used to determine the continuous change in crack velocity in a fracturing polycarbonate modified compact (M-CT) specimen. While the crack velocity measurements, which were made directly from the Cranz-Schardin photographs may not be accurate, the results appear to be in qualitative agreements with those obtained by the more accurate ultrasonic fractography [17] and streaking photography [19].

The small but sharp changes in crack velocities, which are comparable to those reported in [12], were observed in the Charpy specimens [17] which were subjected to severe stress wave effects. As will be shown later, such discontinuous crack velocities was also observed in small hardened 4340 steel and ceramic specimens where the stress wave effect is pronounced.

#### Experimental-Numerical Procedure

The crack tip state of stress of a propagating crack in opaque or optically insensitive material has been determined by photoelastic coating method [21] and the more popular caustic method. An alternate procedure is to combine experimental and numerical techniques by using measured crack extension history interactively with a dynamic finite difference or finite element program in its generation or propagation phase [22]. The latter propagation analysis was used extensively by the Battelle group [23] to study the dynamic crack toughness and arrest characteristics of steel [24] and by one of the authors and his colleague to study the nonlinear fracture response of concrete [25]. The former generation analysis has been used to study the dynamic fracture response of glass [26] and reaction bonded silicon nitride [25].

The above hybrid experimental-numerical procedure was used to determine the  $K_{ID}$  versus  $\dot{a}$  relation for 4340 steel hardened to Rockwell C 44. The dynamic crack extension histories in four wedge-loaded modified double cantilever beam specimens (WL-MDCB), shown in Figure 6 (a), and with a chevron starter notch were measured by a KRAK-GAGE\* and FRACTOMAT.\* Figure 7 shows typical crack extension records of two fracturing 4340 WL-MDCB specimens. The initial and slower crack propagation in the chevron notch specimens is followed by rapid crack propagation and subsequent deceleration. The latter crack

---

\*TTI Division, Hartrum Corp. Chaska, MN.



deceleration is interrupted by a number of short intervals of crack arrest where the average time between each crack arrest coincides with the average transit time of shear wave from the crack tip to the lateral edge of the specimen and back.

Such intermittent crack propagation is more pronounced in the blunt notch 4340 WL-MTDCB specimen, which is heat treated to a hardness of Rockwell C 52. Figure 8 shows the crack extension history with crack arrest intervals indicated by arrow marks. Such intermittent crack arrests, as long as 20 microseconds, were reported by Van Elst [28] and de Graaf [29], who used streaking photography to record continuous crack extension in Robertson type low-carbon steel specimens. Ravi-Chandar et al [7] and Rosakis et al [10] also reported the presence of discontinuous crack velocities in their highly dynamically loaded specimens.

Returning to the hybrid experimental-numerical procedure, an average of the measured crack extension histories, which are shown in Figure 9, without crack arrest of four 4340 steel WL-MTDCB specimens was then used to drive a dynamic finite element code in its generation mode and the dynamic fracture parameters were determined.

Figure 10 shows the  $K_{ID}$  versus crack extension relation as well as the corresponding static stress intensity factor in this high strength 4340 steel WL-MTDCB specimen. Figure 11 shows the  $K_{ID}$  versus  $\dot{a}$  relation for this study as well as that of Rosakis et al [10]. The remarkable agreement between the two independent results could be due in part to the similarities in specimen geometries.

Despite the differences in  $K_{ID}$  versus  $\dot{a}$  relations, a vertical stem in the  $K_{ID}$  versus  $\dot{a}$  relation always existed in the photoelastic polymers and 4340 steel specimens discussed so far. However, limited dynamic fracture studies of

extremely brittle materials, such as glass and structural ceramics [26,27,30], show that  $K_{Im}$  and hence the vertical stem in the  $K_{ID}$  versus  $\dot{a}$  curve does not exist in some materials. Figure 12 shows the  $K_{ID}$  versus  $\dot{a}$  relation of reaction bonded silicon nitride WL-MTDCB specimens loaded to fracture under both static and dynamic conditions. The specimen geometry is identical to that shown in Figure 6 (a) with Figure 6 (b) showing the dynamic loading arrangement. While the crack propagating under static loading had attempted to arrest, as shown in Figure 12, the same crack propagating under dynamic loading showed little tendency for arresting.

## CONCLUSIONS

As profoundly stated by many authors in [3], the controversy regarding the uniqueness or lack thereof in the  $K_{ID}$  versus  $\dot{a}$  relation is far from being settled. While available experimental results indicate that in the absence of stress wave effects, such as in infinitely large fracture specimen under benign loading,  $K_{ID}$  versus  $\dot{a}$  relation may possess a unique  $K_{Im}$  or a vertical stem. Such unique vertical stem is not observed in dynamic fracture specimens of smaller size and/or under dynamic loading.

Comparative study of various experimental data shows that the consistency in data scatter cannot be totally attributed to experimental errors and that the intermittent crack arrest and the discrete changes in crack velocity are caused by the reflected stress wave.

## DISCUSSION

In the pursuit of the above uniqueness controversy, we pose the question "for what reason?" The end use of the sought  $K_{ID}$  versus  $\dot{a}$  relation is as the fourth constitutive equation for estimating the dynamic fracture response of an elastic solid. Limited numerical experiments show that the arrest crack length

of a propagating crack is obviously governed by  $K_{Im}$  [31-34]. For a dynamically loaded specimen or in the presence of severe stress wave effects, however, small differences in  $K_{Im}$  may not cause large differences in the arrest crack length while the same difference in  $K_{Im}$  may cause large differences in arrest crack length in the absence of stress wave effects.

#### ACKNOWLEDGEMENTS

Most of the work reported here was obtained under ONR contract Nos. N00014-76-C-0060 NR 064-478 and N00014-85-K-0187. The authors wish to acknowledge the support and encouragement of Dr. Yapa Rajapakse, ONR, during the course of this investigation. The 4340 steel and ceramic fracture results were obtained under NASA contract NAGW-199.

#### REFERENCES

1. Wells, A. A. and Post, D., "The Dynamic Stress Distribution Surrounding a Running Crack - A Photoelastic Analysis," Proceedings of the Society for Experimental Stress Analysis, Vol. XVI, No. 1, pp. 69-92, 1958.
2. Irwin, G. R., "Discussion," Proceedings of the Society for Experimental Stress Analysis, Vol. XVI, No. 1, pp. 93-96, 1958.
3. International Journal of Fracture, Vol. 27, Nos. 3-4, 1985.
4. Dally, J. W., Fournery, W. L. and Irwin, G. R., "On the uniqueness of the of the stress intensity factor-crack velocity relation," International Journal of Fracture, Vol. 27, Nos. 3-4, pp. 159-168, 1985.
5. Dally, J. W., "Dynamic Photoelastic Studies of Fracture," Experimental Mechanics, Vol. 19, No. 10, pp. 349-367, October 1979.
6. Kalthoff, J. F., Beinert, J. and Winkler, S., "Influence of Dynamic Effect on Crack Arrest," Institut fuer Festkoepermechanik report prepared under Electric Power Research Contract RP 1022-1 IKFM 40412, 1978.
7. Ravi-Chandar, K. and Knauss, W. G., "Processes Controlling the Dynamic Fracture of Brittle Solids," Workshop on Dynamic Fracture, California Institute of Technology, pp. 119-128, February 1983.
8. Kobayashi, A. S. and Mall, S., "Dynamic Fracture Toughness of Homalite-100," Experimental Mechanics, Vol. 18, No. 1, pp. 11-18, January 1978.
9. Kobayashi, A. S. and Mall, S., "Rapid Crack Propagation and Arrest in Polymers," Journal of Polymer Engineering and Science, Vol. 19, No. 2, pp.

131-135 mid-February 1979.

10. Rosakis, A. J., Duffy, J and Freund, L. B., "Dynamic Crack Growth Criteria In Structural Metals," Workshop on Dynamic Fracture, California Institute of Technology, pp. 100-118, February 1983.
11. Kalthoff, J. F., Beinert, J. and Winkler, S., " Measurements of Dynamic Stress Intensity Factors for Fast Running and Arresting Cracks in Double-Cantilever-Beam Specimens," Fast Fracture and Crack Arrest, ASTM STP 627, ed. G. T. Hahn and M. F. Kanninen, pp. 161-176, 1977.
12. Rosakis, A. J. and Zehnder, A. T., "On the dynamic fracture of metals," International Journal of Fracture, Vol. 27, pp. 169-186, 1985.
13. Smith, C. W., "A Study of Crack-tip Nonlinearities in Frozen-stress Fields," Experimental Mechanics, Vol. 18, No. 8, pp. 309-315, August 1978.
14. Metcalf, J. T. and Kobayashi, Takao, "Comparison of Crack Behavior in Homalite 100 and Aradite B," Crack Arrest Methodology and Applications, ASTM STP 711, ed. G. T. Hahn and M. F. Kanninen, pp. 128-145, 1980.
15. Knauss, W. G. and Ravi-Chandar, K., "Some basic problems in stress-wave dominated fracture," International Journal of fracture, Vol. 27, pp. 127-143, 1985.
16. Kerkhof, F., "Ultrasonic Fractography," Proceedings of 3rd International Congress on High-Speed Photography, Butterworth, London, pp. 194-200, 1957.
17. Takahashi, K., Matsushige, K. and Sakurada, Y., "Precise evaluation of fast fracture velocities in acrylic polymers at the slow-to-fast transition," Journal of Material Science, Vol. 19, pp. 4026-4034, 1984.
18. Bradley, W. B. and Kobayashi, A. S., "An Investigation of Propagating Cracks Dynamic Photoelasticity," Experimental Mechanics, Vol. 10, No. 3, pp. 106-113, March 1970.
19. Kobayashi, A. S., Seo, K, Jou, J.-Y. and Urabe, Y., "Dynamic Analyses of Homalite-100 and Polycarbonate Modified Compact-Tension Specimens," Experimental Mechanics, Vol. 20, No. 9, pp. 301-308, September 1980.
20. Mall, S., Kobayashi, A. S. and Urabe, Y., "Dynamic Photoelastic and Dynamic Finite-element Analyses of Dynamic-tear-test Specimens," Experimental Mechanics, Vol. 18, NO. 12, pp. 449-456, December 1978.
21. Kobayahsi, Takao and Dally, J. W., "Dynamic Photoelastic Determination of the a.-K relation for 4340 Alloy Steel," Crack Arrest Methodology and Applications, "ASTM STP 711, ed. by G. T. Hahn and M. F. Kanninen, pp. 189-210, 1982.
22. Kobayashi, A. S., "Dynamic Fracture Analysis by Dynamic Finite Element Method-Generation and Propagation Analyses," Nonlinear and Dynamic Fracture Mechanics, ed. by N. Perrone and S. N. Atluri, ASME AMD-35, pp. 19-35, 1979.
23. Kanninen, M. F., Gehlen, P. C., Barnes, C. R., Hoagland, R. G., Hahn, G. T.

- and Popelar, C. H., "Dynamic Crack Propagation Under Impact Loading, Nonlinear and Dynamic Fracture Mechanics, ed. by N. Perrone and S. N. Atluri, ASME AMD-35, pp. 189-200, 1979.
24. Hahn, G. T., Hoagland, R. G., Lereim, J., Markworth, A. J. and Rosenfield, A. R., "Fast Fracture Toughness and Crack Arrest Toughness of Reactor Pressure Vessel Steel," Crack Arrest Methodology and Applications, ASTM STP 711, ed. by G. T. Hahn and M. F. Kanninen, pp. 289-320, 1980.
  25. Cho, K.-Z., Kobayashi, A. S., Hawkins, N. M., Barker, D. B., and Jeang, P. L., ASCE Journal of Engineering Mechanics, Vol. 110, No. 8, pp. 1174-1184, August 1984.
  26. Kobayashi, A. S., Emery, A. F. and Liaw, B. M., "Dynamic Fracture Toughness of Glass," Fracture Mechanics of Ceramics, Vol. 6, ed. by R. C. Bradt, A. G. Evans, D. P. H. Hasselman and F. F. Lange, Plenum Press, pp. 47-62, 1983.
  27. Kobayashi, A. S., Emery, A. F. and Liaw, B. M., "Dynamic Fracture Toughness of Reaction Bonded Silicon Nitride," Journal of American Ceramic Society, Vol. 66, No. 2, pp. 151-155, February 1983.
  28. Van Elst, H. C., "The Intermittent Propagation of Brittle Fracture," Transaction of the Metallurgical Society of AIME, Vol. 230, pp. 460-469, April 1964.
  29. De Graaf, J. G. A., "Investigation of Brittle Fracture in Steel by Means of Ultra High Speed Photography," Applied Optics, Vol. 3, No. 11, pp. 1223-1229, November 1964.
  30. Liaw, B. M., Kobayashi, A. S. and Emery, A. F., "Effect of Loading Rate on Dynamic Fracture of Reaction Bonded Silicon Nitride," to be published in ASTM STP.
  31. Cheverton, R. D., Gehlen, P. C., Hahn, G. T. and Iskander, S. K., "Application of Crack Arrest Theory to a Thermal Shock Experiment," Crack Arrest Methodology and Applications, ASTM STP 711, ed. by G. T. Hahn and M. F. Kanninen, pp. 392-418, 1980.
  32. Popelar, C. H., Gehlen, P. C. and Kanninen, M. F., "Dynamic Crack Propagation in Precracked Cylindrical Vessels Subjected to Shock Loading," ASME Journal of Pressure Vessel Technology, Vol. 103, pp. 155-159, 1981.
  33. Nishioka, T. and Atluri, S. N., "Numerical Analysis of Dynamic Crack Propagation: Generation and Prediction Studies," Engineering Fracture Mechanics, Vol. 16, No. 1, pp. 303-332, 1982.
  34. Hodulak, L., Kobayashi, A. S. and Emery, A. F., "Influence of Dynamic Fracture Toughness on Dynamic Crack Propagation," Engineering Fracture Mechanics, Vol. 13, No. 1, pp. 84-93, 1980.

HOMALITE-100 DTT-4. MCT-1. RDCB-6

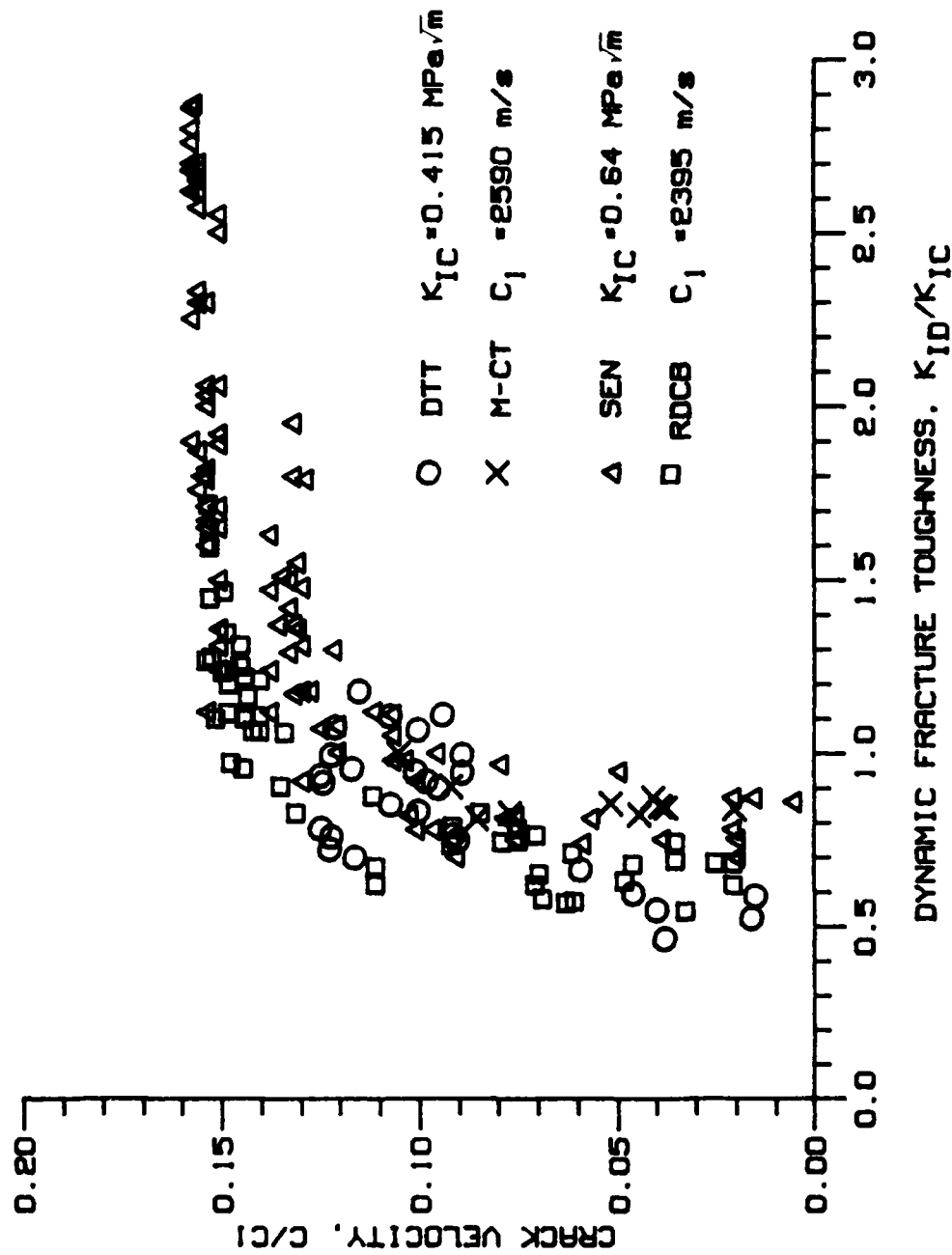


FIGURE 1. DYNAMIC FRACTURE TOUGHNESS VERSUS CRACK VELOCITY  
RELATION. HOMALITE-100

POLYCARBONATE DTT-8, SEN-5, RDCB-2

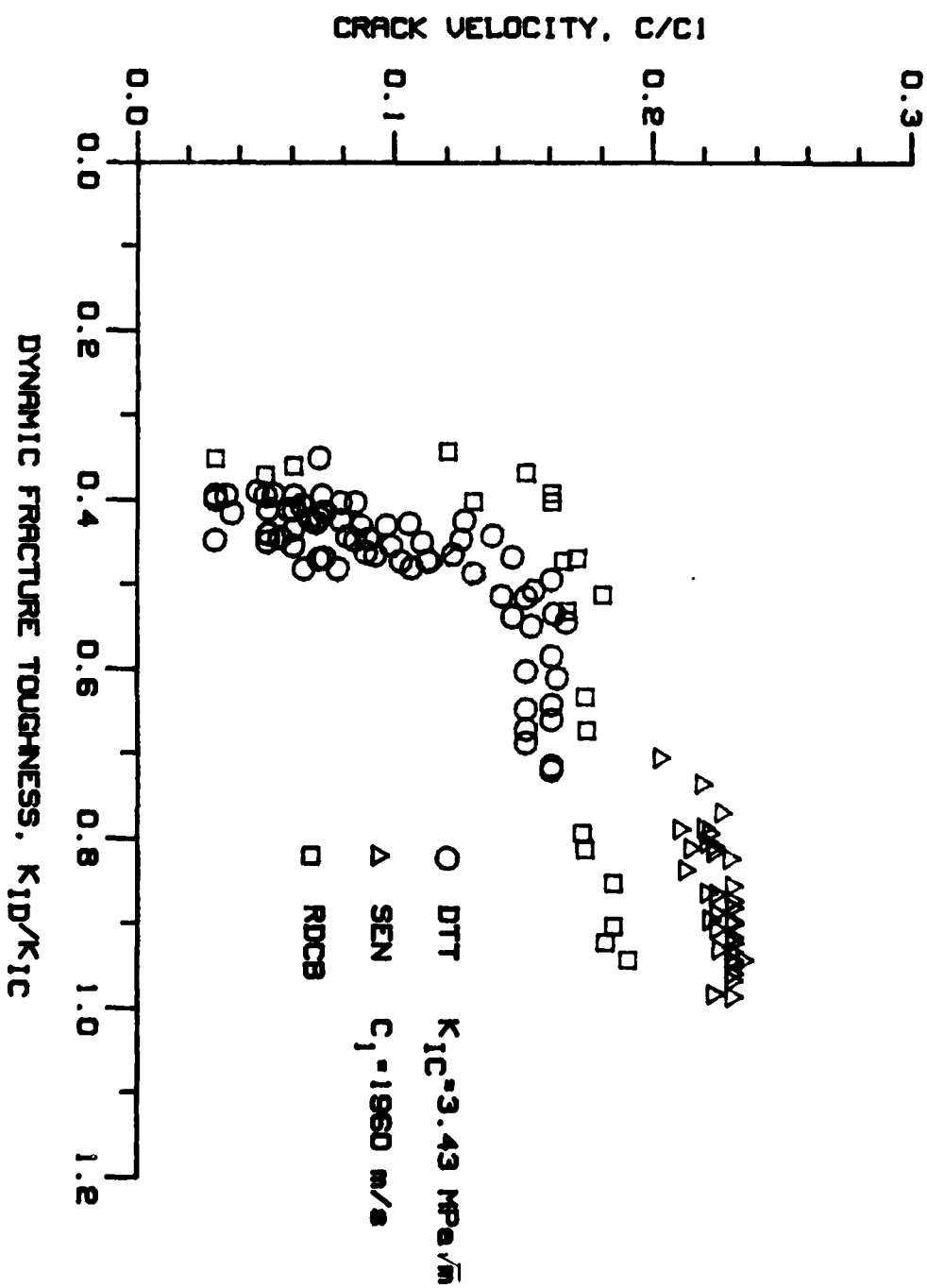


FIGURE 2. DYNAMIC FRACTURE TOUGHNESS VERSUS CRACK VELOCITY RELATION. POLYCARBONATE

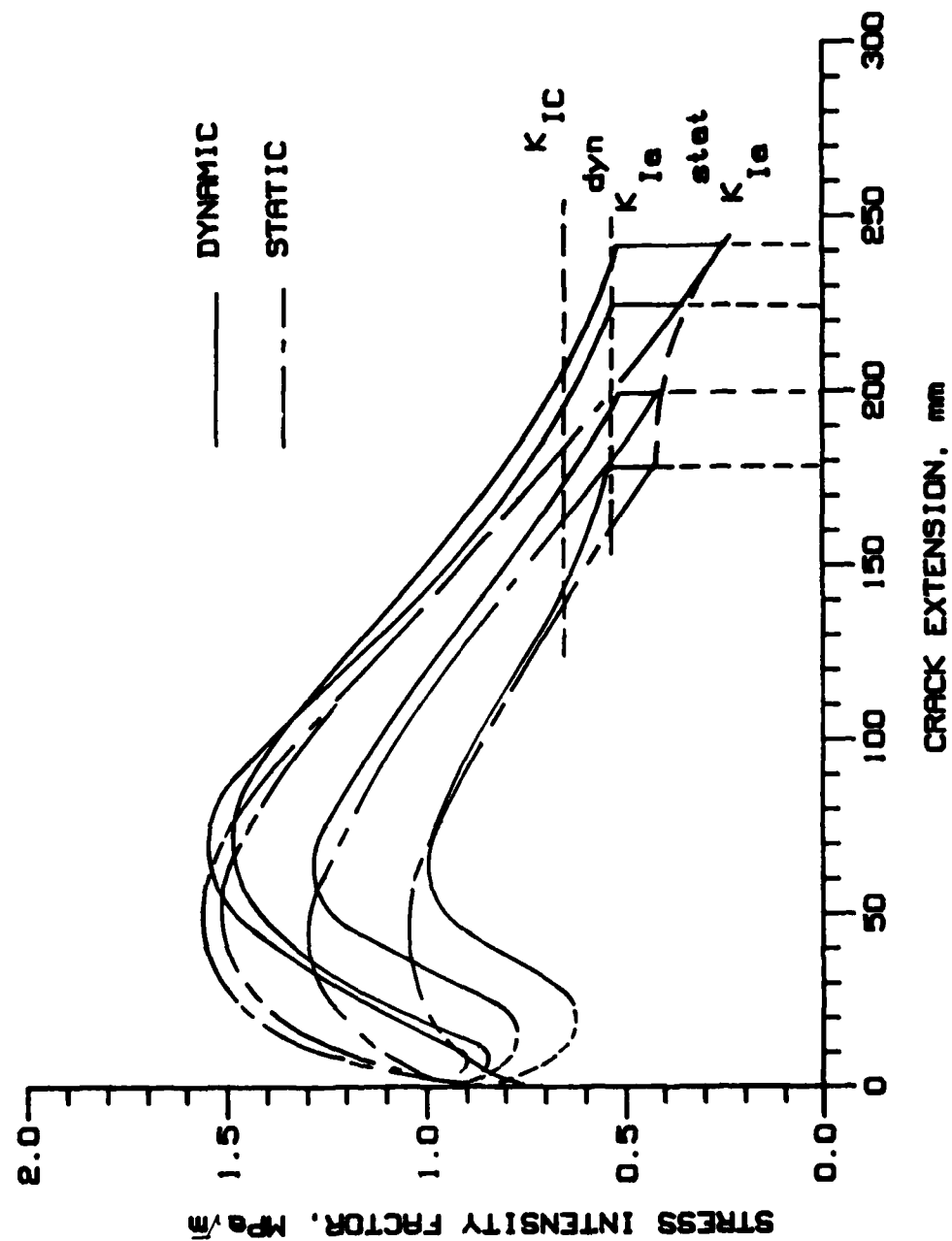


FIGURE 3. STRESS INTENSITY FACTOR VERSUS CRACK LENGTH  
HOMALITE-100 SEN SPECIMENS.



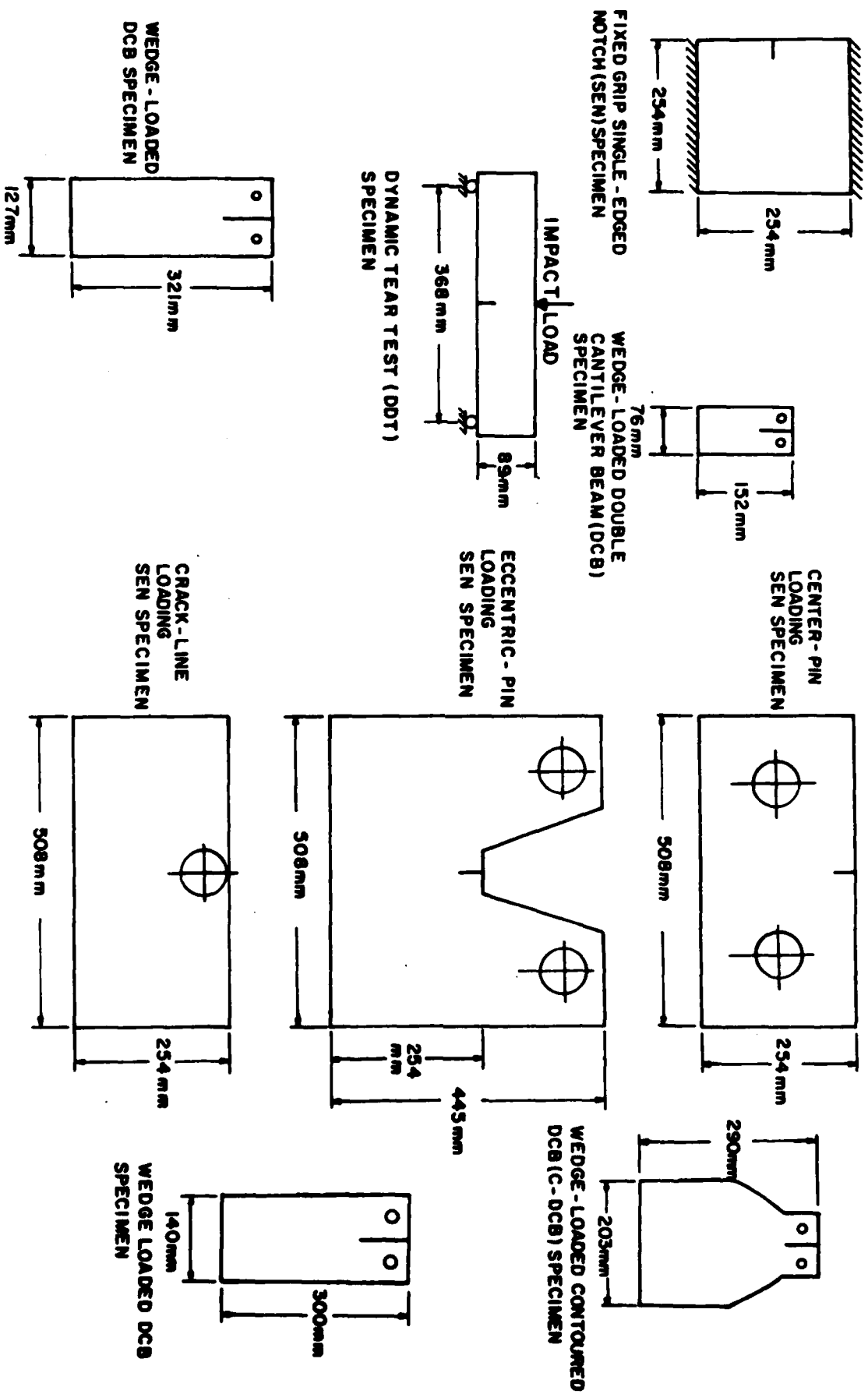
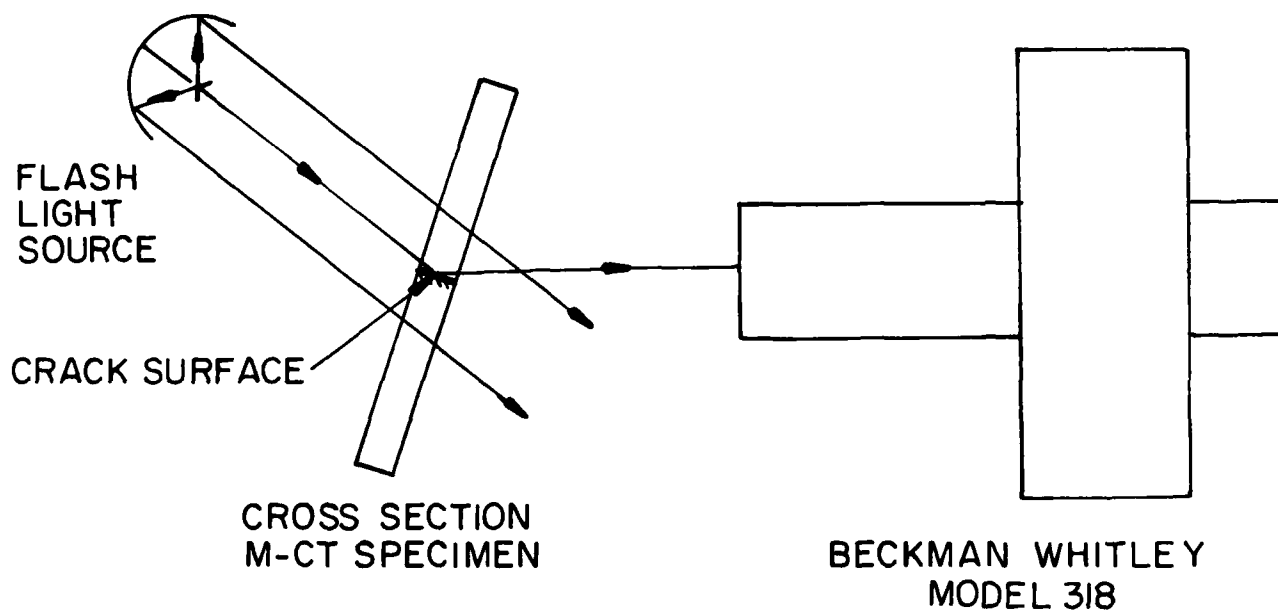


FIGURE 4. SPECIMENS USED IN FRACTURE DYNAMIC ANALYSIS



EXPERIMENTAL SET UP FOR STREAKING PHOTOGRAPHY

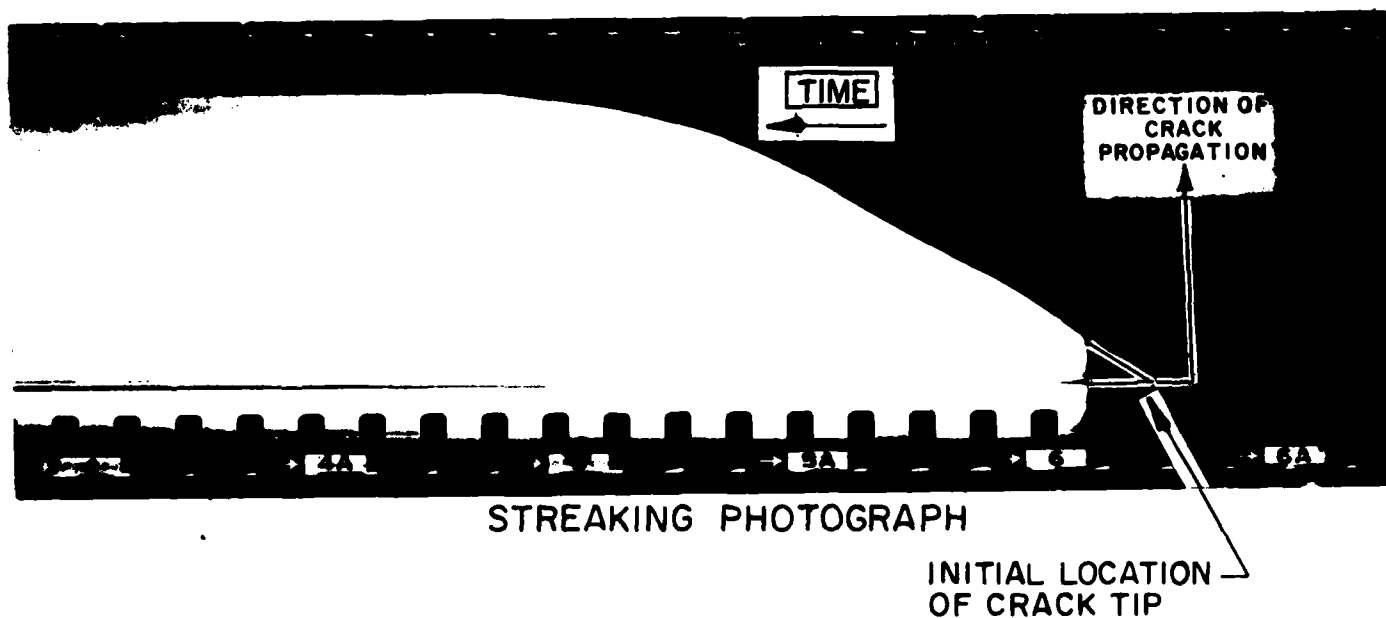
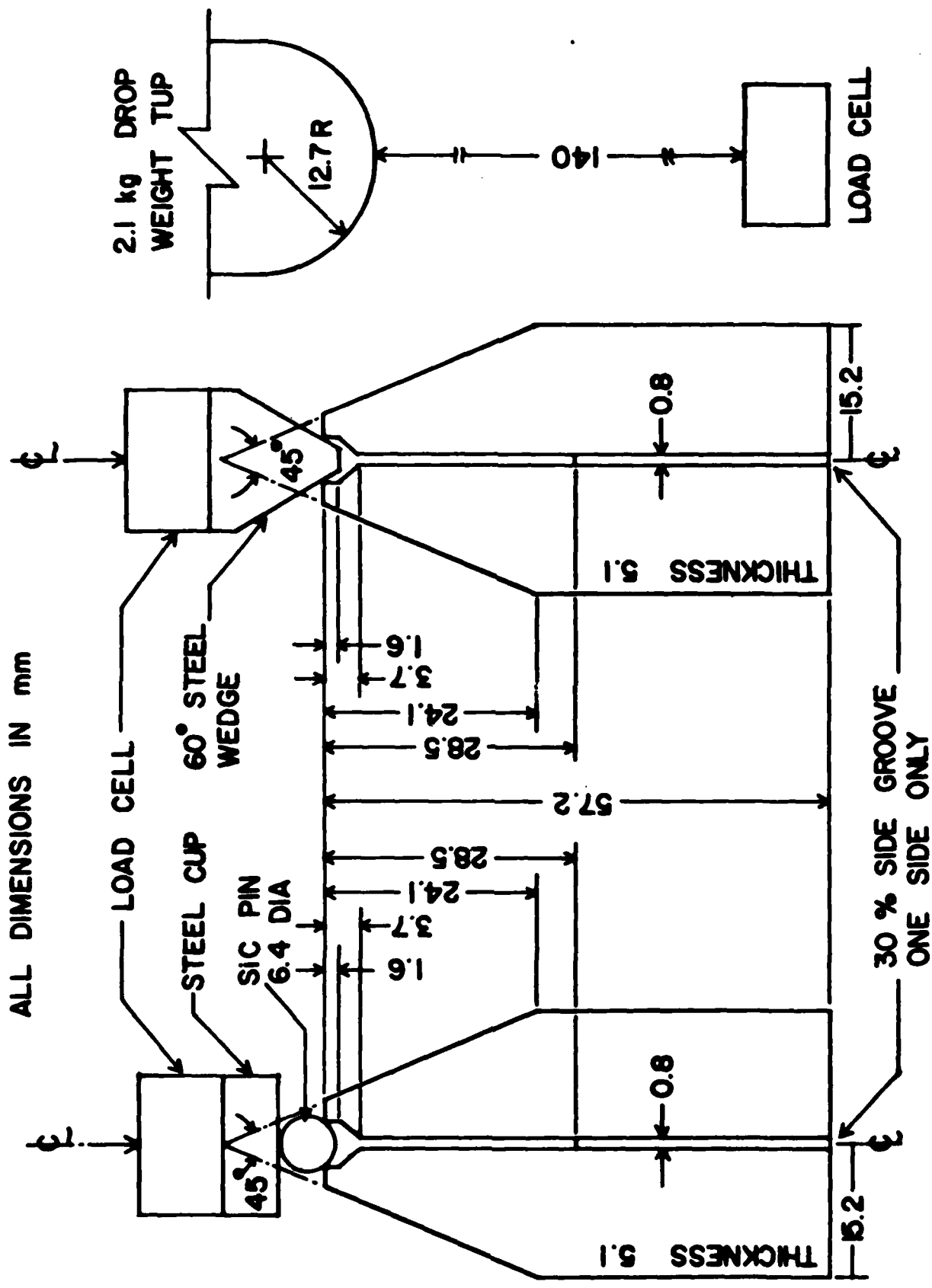


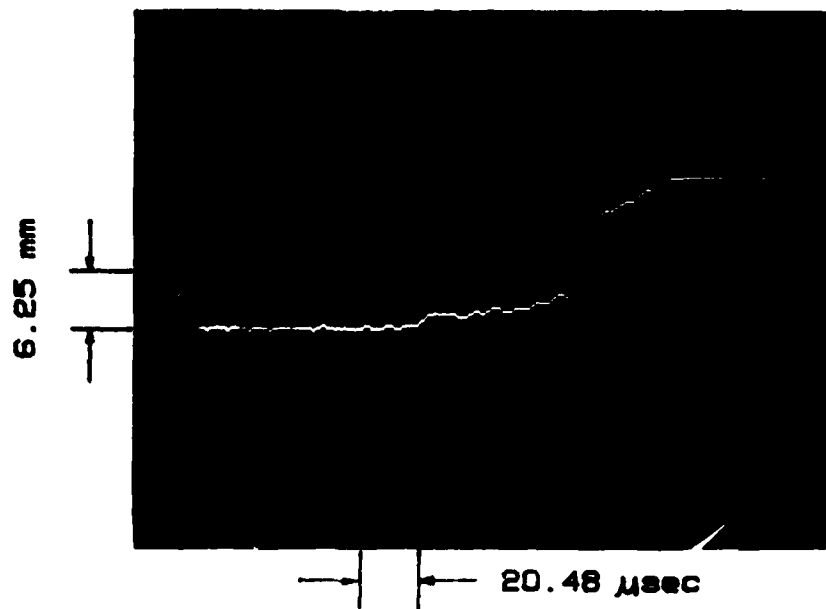
FIGURE 5. STREAKING PHOTOGRAPH OF A PROPAGATING CRACK TIP  
IN A POLYCARBONATE M-CT SPECIMEN (THICKNESS 6.4mm)



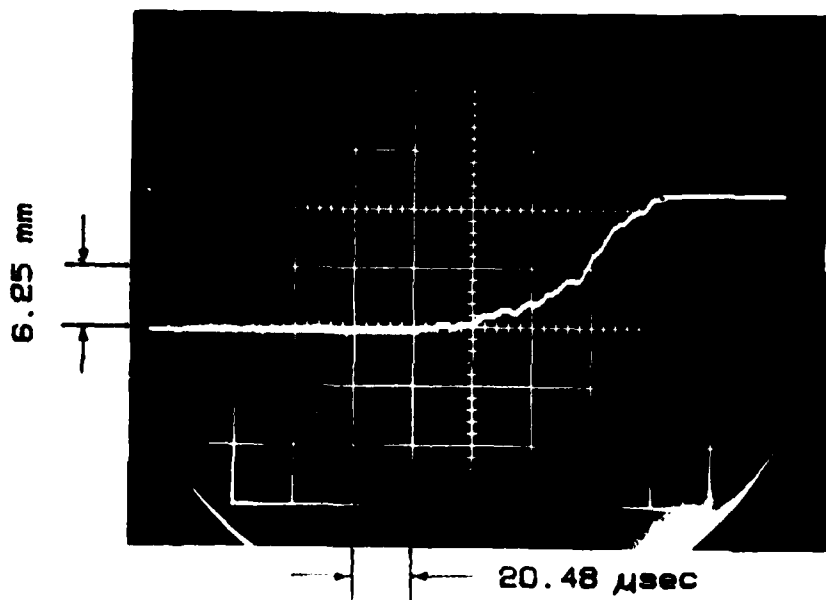
(a) STATIC LOADING

(b) IMPACT LOADING

FIGURE 6. WL-MTDCB SPECIMEN (4340 STEEL AND REACTION BONDED SILICON NITRIDE).



(a) KH070785



(b) KH071585

FIGURE 7. CRACK EXTENSION VERSUS TIME, CHEVRON NOTCHED 4340 STEEL WL-MTDCB SPECIMEN.

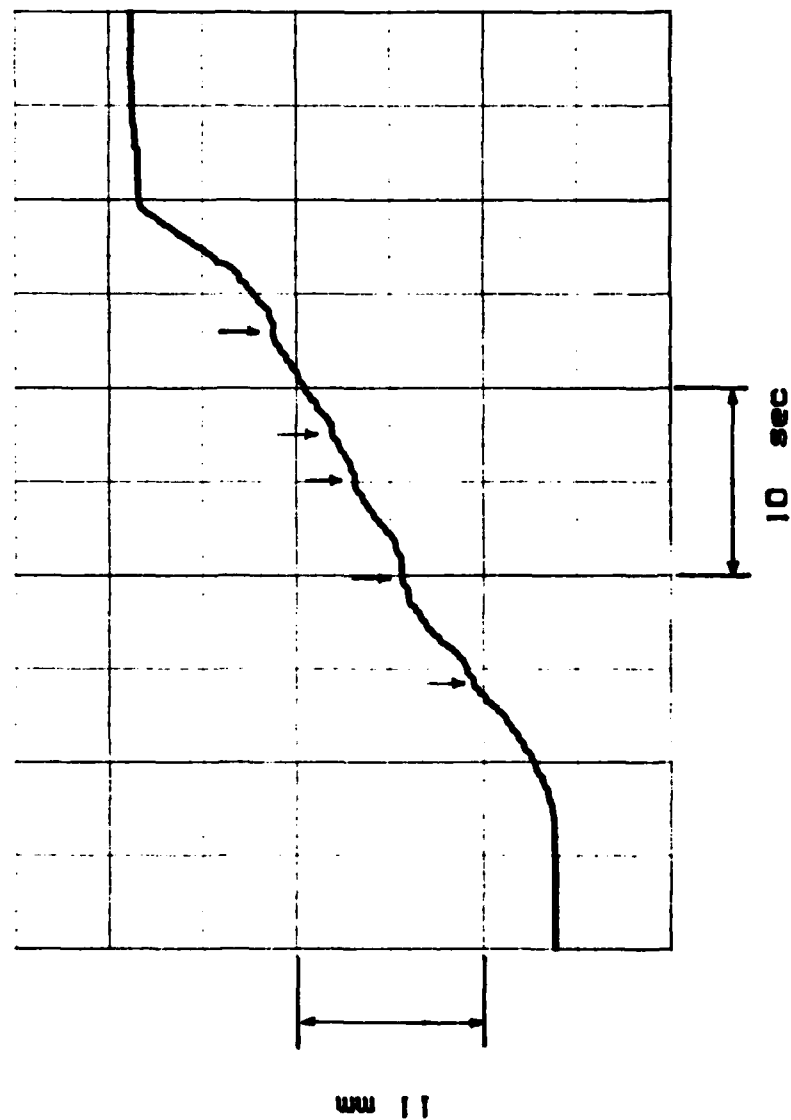


FIGURE 8. CRACK EXTENSION VERSUS TIME, BLUNT NOTCH 4340  
STEEL WL-MTDCB SPECIMEN.

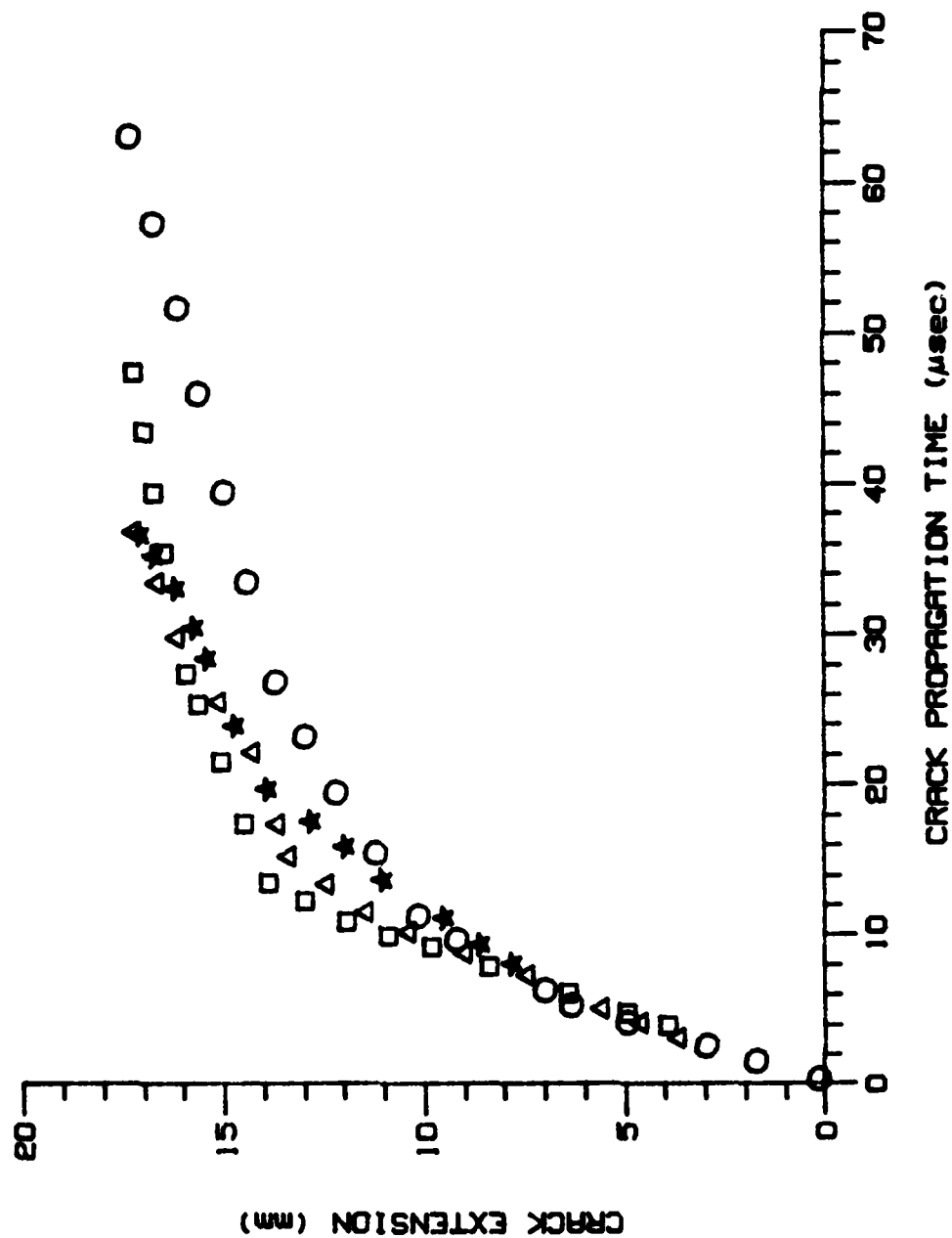


FIGURE 9. CRACK EXTENSION VERSUS TIME. CHEVRON NOTCHED  
4340 STEEL WL-MTDCB SPECIMENS.

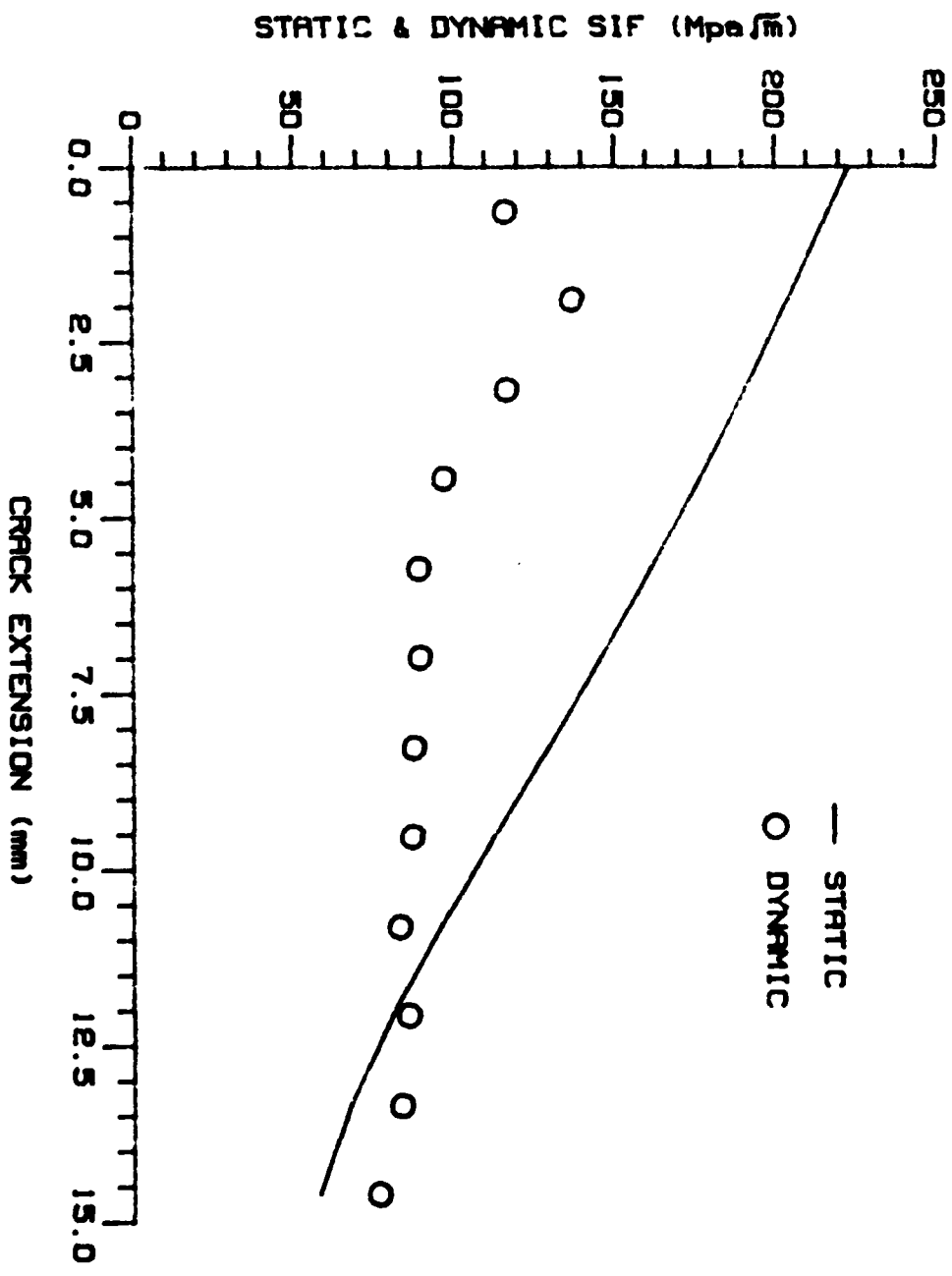


FIGURE 10. STRESS INTENSITY FACTORS VERSUS CRACK EXTENSION  
CHEVRON NOTCH 4340 STEEL WL-MTDCB SPECIMEN.

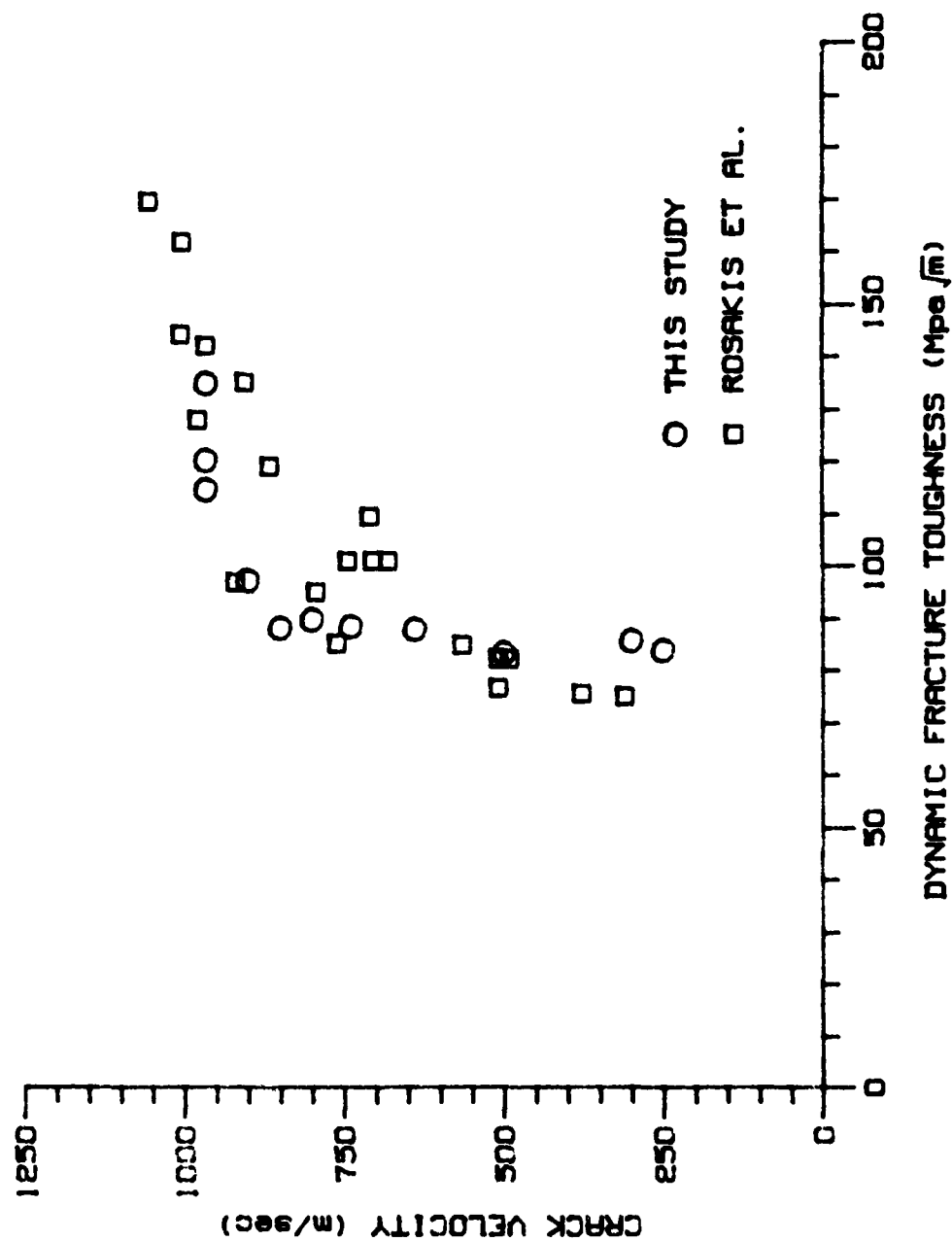


FIGURE 11. DYNAMIC FRACTURE TOUGHNESS VERSUS CRACK VELOCITY RELATIONS OF 4340 STEEL



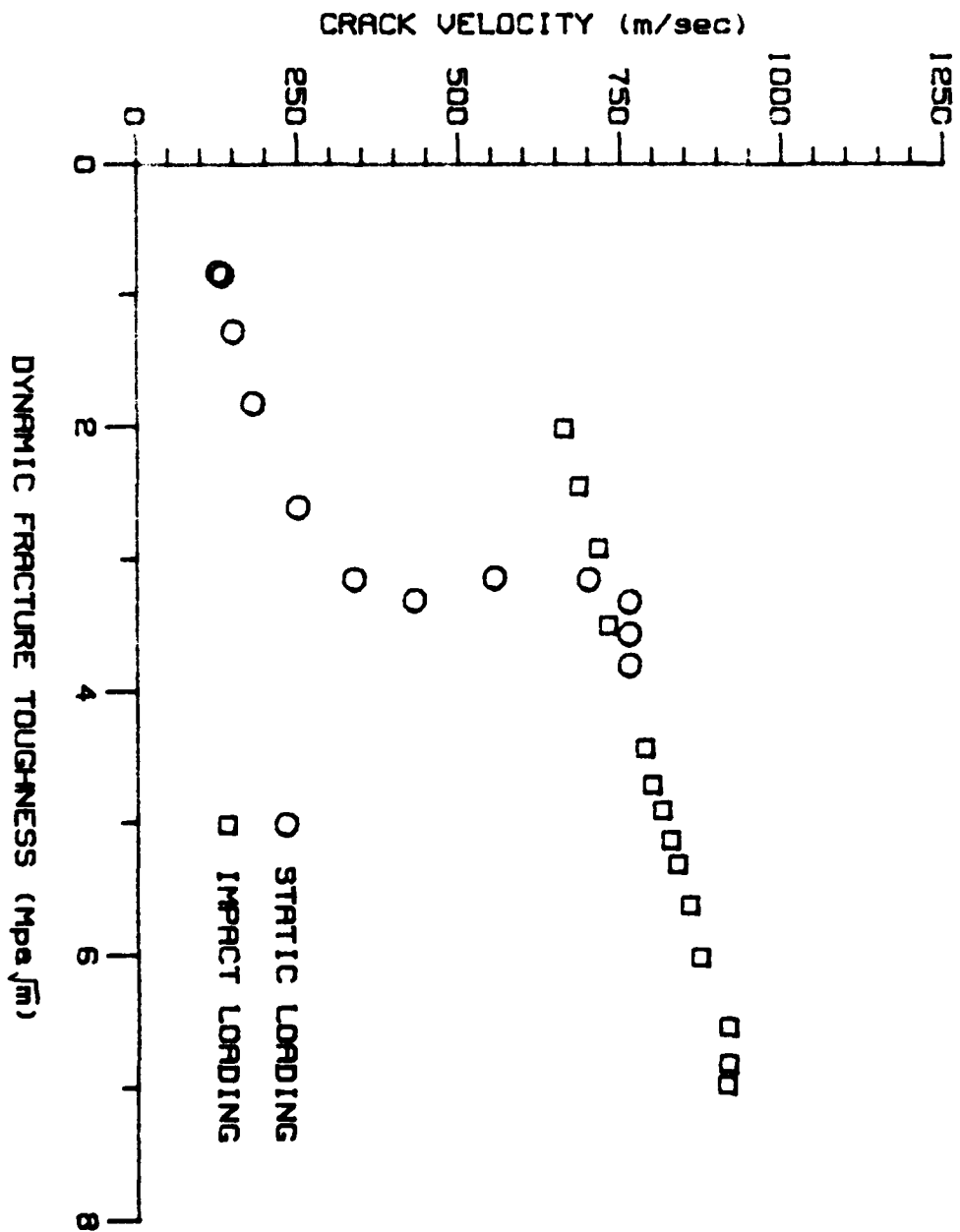


FIGURE 12. DYNAMIC FRACTURE TOUGHNESS VERSUS CRACK VELOCITY RELATIONS OF BLUNT NOTCH RBSN WL-MTDCB SPECIMENS.

Office of Naval Research  
800 N. Quincy Street  
Arlington, VA 22217  
Attn: Code 432 (4 copies)

Office of Naval Research  
800 N. Quincy Street  
Arlington, VA 22217  
Attn: Code 431

Defense Documentation Center (12 copies)  
Cameron Station  
Alexandria, VA 22314

Naval Research Laboratory  
Washington, DC 20375  
Attn: Code 6000

Naval Research Laboratory  
Washington, DC 20375  
Attn: Code 6300

Naval Research Laboratory  
Washington, DC 20375  
Attn: Code 6380

Naval Research Laboratory  
Washington, DC 20375  
Attn: Code 5800

Naval Research Laboratory  
Washington, DC 20375  
Attn: Code 6390

Naval Research Laboratory  
Washington, DC 20375  
Attn: Code 2620

David W. Taylor Naval Ship Research  
and Development Center  
Annapolis, MD 21402  
Attn: Code 28

David W. Taylor Naval Ship Research  
and Development Center  
Annapolis, MD 21402  
Attn: Code 2812

David W. Taylor Naval Ship Research  
and Development Center  
Annapolis, MD 21402  
Attn: Code 2814

Commander  
Naval Sea Systems Command  
Washington, D.C. 20362  
Attn: Code 05R26

Commander  
Naval Sea Systems Command  
Washington, D.C. 20362  
Attn: Code 09B31

Commander  
Naval Sea Systems Command  
Washington, D.C. 20362  
Attn: Code 55Y

Commander  
Naval Sea Systems Command  
Washington, D.C. 20362  
Attn: Code 55Y2

Commander  
Naval Air Systems Command  
Washington, D.C. 20361  
Attn: Code 030

Commander  
Naval Air Systems Command  
Washington, D.C. 20361  
Attn: Code 7226

Commander  
Naval Air Systems Command  
Washington, D.C. 20361  
Attn: Code 310A

Commander  
Naval Air Systems Command  
Washington, D.C. 20361  
Attn: Code 310B

U.S. Naval Academy  
Mechanical Engineering Department  
Annapolis, MD 21402

Naval Postgraduate School  
Monterey, CA 93940  
Attn: Technical Library

Mr. Jerome Persh  
Staff Specialist for Materials  
and Structures  
QUSDE&E, The Pentagon  
Room 3D1089  
Washington, D.C. 20301

Dr. Harold Liebowitz, Dean  
School of Engineering and Applied Science  
George Washington University  
Washington, D.C. 20052

Professor J.L. Sanders  
Harvard University  
Division of Applied Science  
Cambridge, MA 02138

Professor G. T. Hahn  
Vanderbilt University  
Department of Mechanical  
& Materials Engineering  
Nashville, TN 37235

Professor G. C. M. Sih  
Lehigh University  
Institute of Fracture and Solid Mechanics  
Bethlehem, PA 18015

Professor Albert S. Kobayashi  
Mechanical Engineering, FU-10  
University of Washington  
Seattle, WA 98195

Professor L.B. Freund  
Brown University  
Division of Engineering  
Providence, RI 02912

Professor B. Budiansky  
Harvard University  
Division of Applied Sciences  
Cambridge, MA 02138

Professor S. N. Atluri  
Georgia Institute of Technology  
School of Engineering and Mechanics  
Atlanta, GA 30332

Professor P. G. Hodge, Jr.  
University of Minnesota  
Department of Aerospace Engineering  
and Mechanics  
Minneapolis, MN 55455

Professor J. D. Achenbach  
Northwestern University  
Department of Civil Engineering  
Evanston, IL 60201

David W. Taylor Naval Ship Research  
and Development Center  
Bethesda, MD 20084  
Attn: Code 1700

David W. Taylor Naval Ship Research  
and Development Center  
Bethesda, MD 20084  
Attn: Code 1720

David W. Taylor Naval Ship Research  
and Development Center  
Bethesda, MD 20084  
Attn: Code 1720.4

Naval Air Development Center  
Warrminster, PA 18974  
Attn: Code 6063

Naval Air Development Center  
Warrminster, PA 18974  
Attn: Code 6043

Naval Surface Weapons Center  
White Oak, MD 20910  
Attn: Code R30

Naval Surface Weapons Center  
Dahlgren, VA 22448  
Attn: Technical Library

Naval Underwater Systems Center  
New London, CT 06320  
Attn: Code 44

Naval Underwater Systems Center  
Newport, RI 02841  
Attn: Technical Library

Naval Weapons Center  
China Lake, CA 93555  
Attn: Technical Library

NRL/Underwater Sound Reference Detachment  
Orlando, FL 32856  
Attn: Technical Library

Chief of Naval Operations  
Department of the Navy  
Washington, DC 20350  
Attn: Code OP-098

Commander  
Naval Sea Systems Command  
Washington, D.C. 20362  
Attn: Code 05R25

Professor F. A. McClintock  
Massachusetts Institute of Technology  
Department of Mechanical Engineering  
Cambridge, MA 02139

Professor D. M. Parks  
Massachusetts Institute of Technology  
Department of Mechanical Engineering  
Cambridge, MA 02139

Dr. M. F. Kanninen  
Southwest Research Institute  
Post Office Drawer 28510  
6220 Culebra Road  
San Antonio, TX 78284

Professor F. P. Chiang  
State University of New York  
at Stony Brook  
Dept. of Mechanical Engineering  
Stony Brook, NY 11794

Professor S. S. Wang  
University of Illinois  
Dept. of Theoretical  
& Applied Mechanics  
Urban, IL 61801

Professor Y. Weitsman  
Texas A&M University  
Civil Engineering Department  
College Station, TX 77843

Professor I. M. Daniel  
Illinois Institute of Technology  
Dept. of Mechanical Engineering  
Chicago, IL 60616

Professor C. T. Sun  
Purdue University  
School of Aeronautics & Astronautics  
W. Lafayette, IN 47907

Professor J. Averbuch  
Drexel University  
Dept. of Mechanical Engr. & Mechanics  
Philadelphia, PA 19104

Professor J. Rose  
Drexel University  
Dept. of Mechanical Engr. & Mechanics  
Philadelphia, PA 19104

Professor G. J. Dvorak  
Rensselaer Polytechnic Institute  
Department of Civil Engineering  
Troy, New York 12181

Dr. R. M. Christensen  
Lawrence Livermore National Laboratory  
Chemistry & Material Science Department  
P.O. Box 80P  
Livermore, CA 94550

Prof. J. R. Rice  
Harvard University  
Division of Applied Sciences  
Cambridge, MA 02138

Dr. M. L. Williams  
University of Pittsburgh  
Dean of Engineering  
Pittsburgh, PA 15261

Dr. R. H. Gallagher  
University of Arizona  
Dean of Engineering  
Tucson, AZ 85721

Dr. D. C. Drucker  
University of Florida  
Div. of Engineering Science  
& Mechanics  
Gainesville, FL 32611

Dean B. A. Boley  
Northwestern University  
Department of Civil Engineering  
Evanston, IL 60201

MR:bk:64

Unclassified

SECURITY CLASSIFICATION OF THIS PAGE (When Data Entered)

REPORT DOCUMENTATION PAGE		READ INSTRUCTIONS BEFORE COMPLETING FORM
1. REPORT NUMBER UWA/DME/TR-85/53	2. GOVT ACCESSION NO. <i>AD-A159382</i>	3. RECIPIENT'S CATALOG NUMBER
4. TITLE (and Subtitle) Dynamic Fracture Toughness		5. TYPE OF REPORT & PERIOD COVERED UWA/DME/TR-85/53
		6. PERFORMING ORG. REPORT NUMBER
7. AUTHOR(s) A. S. Kobayashi, M. Ramulu, M. S. Dadkhah, K.-H. Yang and B. S. J. Kang		8. CONTRACT OR GRANT NUMBER(s) N00014-85-K-0187
9. PERFORMING ORGANIZATION NAME AND ADDRESS Dept. of Mechanical Engineering, FU-10 University of Washington Seattle, Washington 98195		10. PROGRAM ELEMENT, PROJECT, TASK AREA & WORK UNIT NUMBERS
11. CONTROLLING OFFICE NAME AND ADDRESS Office of Naval Research Arlington, VA 22217		12. REPORT DATE August 1985
		13. NUMBER OF PAGES
14. MONITORING AGENCY NAME & ADDRESS (if different from Controlling Office)		15. SECURITY CLASS. (of this report) Unclassified
		15a. DECLASSIFICATION/DOWNGRADING SCHEDULE
16. DISTRIBUTION STATEMENT (of this Report)  Unlimited		
<div style="border: 1px solid black; padding: 5px; display: inline-block;"> <b>DISTRIBUTION STATEMENT A</b>            Approved for public release;            Distribution Unlimited         </div>		
17. DISTRIBUTION STATEMENT (of the abstract entered in Block 20, if different from Report)		
18. SUPPLEMENTARY NOTES		
19. KEY WORDS (Continue on reverse side if necessary and identify by block number) Dynamic fracture, dynamic photoelasticity, dynamic caustics, dynamic fracture toughness, dynamic crack arrest stress intensity factor		
20. ABSTRACT (Continue on reverse side if necessary and identify by block number) Dynamic fracture toughness versus crack velocity relations of Homalite-100, polycarbonate, hardened 4340 steel and reaction bonded silicon nitride are reviewed and discrepancies with published data and their probable causes are discussed. Data scatter in published data are attributed in part to the observed fluctuations in crack velocities. The results reaffirmed our previous conclusion that the dynamic fracture toughness versus crack velocity relation is specimen dependent and that the dynamic arrest stress intensity factor is not a unique material property.		

DD FORM 1473  
1 JAN 73

EDITION OF 1 NOV 65 IS OBSOLETE  
S/N 0102-014-6601

Unclassified

SECURITY CLASSIFICATION OF THIS PAGE (When Data Entered)

**END**

**FILMED**

**11-85**

**DTIC**